

ARTICLE



Dissimilatory nitrate reduction by a freshwater cable bacterium

Ugo Marzocchi^{1,2,3}✉, Casper Thorup^{2,4}, Ann-Sofie Dam^{2,4}, Andreas Schramm^{2,4} and Nils Risgaard-Petersen^{2,4,5}

© The Author(s), under exclusive licence to International Society for Microbial Ecology 2021

Cable bacteria (CB) are filamentous Desulfobulbaceae that split the energy-conserving reaction of sulfide oxidation into two half reactions occurring in distinct cells. CB can use nitrate, but the reduction pathway is unknown, making it difficult to assess their direct impact on the N-cycle. Here we show that the freshwater cable bacterium *Ca. Electronema* sp. GS performs dissimilatory nitrate reduction to ammonium (DNRA). ¹⁵NO₃⁻-amended sediment with *Ca. Electronema* sp. GS showed higher rates of DNRA and nitrite production than sediment without *Ca. Electronema* sp. GS. Electron flux from sulfide oxidation, inferred from electric potential (EP) measurements, matched the electron flux needed to drive CB-mediated nitrate reduction to nitrite and ammonium. *Ca. Electronema* sp. GS expressed a complete *nap* operon for periplasmic nitrate reduction to nitrite, and a putative octaheme cytochrome c (pOCC), whose involvement in nitrite reduction to ammonium remains to be verified. Phylogenetic analysis suggests that the capacity for DNRA was acquired in multiple events through horizontal gene transfer from different organisms, before CB split into different salinity niches. The architecture of the nitrate reduction system suggests absence of energy conservation through oxidative phosphorylation, indicating that CB primarily conserve energy through the half reaction of sulfide oxidation.

The ISME Journal (2022) 16:50–57; <https://doi.org/10.1038/s41396-021-01048-z>

INTRODUCTION

Cable bacteria (CB) are centimeter-long filamentous Desulfobulbaceae able to split the energy-conserving reaction of sulfide oxidation into two redox half reactions: anodic sulfide oxidation and cathodic oxygen reduction, and to distribute these among distinct cells [1]. This is possible as all cells in the filament are interlinked by highly conductive strings [1, 2], so that cells with access to sulfide can perform anodic sulfide oxidation donating electrons to the strings, whereas cells with access to oxygen can accept electrons from the strings and perform cathodic oxygen reduction. The overall metabolic process was first discovered in marine sediments [3] and is named electrogenic sulfide oxidation (e-SOx) [4]. Since their discovery, CB and e-SOx have been found in diverse aquatic environments, such as marine, brackish, and freshwater sediments [5–7], where they can significantly influence the cycling of major elements such as sulfur, iron, oxygen, and carbon [8–10]. Although the geochemical imprint of CB in the sediment has been well documented in intact and CB-enriched sediment incubations, our current inability to grow pure cultures represents a major limitation to address some of the fundamental questions on the CB's physiology and on the biochemical basis of their metabolic pathways.

Using sediment enrichments, it was demonstrated that CB can use nitrate or nitrite as an electron acceptor to sustain e-SOx in the absence of oxygen [11, 12]. However, the exact nitrate reduction pathway by CB remains, to date, unknown. Experiments conducted on riverine sediment show that CB can promote dissimilatory nitrate reduction to ammonium (DNRA). Such stimulation of DNRA activity appears, at the present, to be only an indirect effect of e-SOx activity, that via promoting the

dissolution of FeS minerals, stimulates Fe²⁺ and/or H₂S driven DNRA performed by other chemotrophs [13].

Recent CB genome sequencing reported the presence of genes encoding the periplasmic reductase NapAB that catalyzes the reduction of nitrate to nitrite [14]. From incubation experiments, it can be deduced that marine CB can reduce nitrite, however, the absence of e-SOx when N₂O was provided as the sole electron acceptor suggested that CB lack of a full denitrification pathway [12]. Typical, *nir* or *nrf*-type, nitrite reductases are absent in CB genomes, but a putative octaheme cytochrome c (pOCC) homologous to a OCC previously found in an orange sulfur bacteria (*Ca. Maribeggiatoa* sp.) is encoded in the most complete CB genomes [14]. There are indications that OCC in *Ca. Maribeggiatoa* sp. can catalyze the reduction of nitrite to ammonium in vitro [15, 16]. Hence a possible pathway for nitrate reduction in CB is nitrate reduction to nitrite followed by nitrite reduction to ammonium, i.e., DNRA.

In the present study, we applied ¹⁵N tracing techniques in CB-enriched sediment to test the hypothesis that CB performs DNRA. To better pinpoint the measured NO₃⁻ reduction processes to e-SOx by CB, we (i) used a clonal enrichment of the freshwater CB strain *Ca. Electronema* sp. GS, (ii) simplified the prokaryotic community (including the removal of residual CB) by heat-treatment of the sediment prior to the inoculation with CB, and (iii) calculated a nitrogen-electrons mass-balance by comparing rates of nitrite production and DNRA with the electric potentials (EPs) that developed in the sediment due to e-SOx activity [12]. In addition, we identified candidate genes for DNRA in the genome of this CB strain [14] and assessed their expression levels along

¹Department of Chemistry, Vrije Universiteit Brussel, Brussel, Belgium. ²Center for Electromicrobiology, Section for Microbiology, Department of Biology, Aarhus University, Aarhus, Denmark. ³Center for Water Technology (WATEC), Department of Biology, Aarhus University, Aarhus, Denmark. ⁴Center for Geomicrobiology, Section for Microbiology, Department of Biology, Aarhus University, Aarhus, Denmark. ⁵Section of Aquatic Biology, Department of Biology, Aarhus University, Aarhus, Denmark. ✉email: ugomar@bio.au.dk

Received: 1 May 2020 Revised: 10 June 2021 Accepted: 23 June 2021

Published online: 2 July 2021

with that of non-CB nitrite reductase genes in the sediment incubations by metatranscriptomic analysis.

MATERIALS AND METHODS

Ca. Electronema sp. GS sediment enrichment and incubation

Sediment was collected from Vennelyst Sø, a freshwater lake at Aarhus University Campus (Aarhus, Denmark). Shortly after collection, the sediment was transported to the laboratory, sieved through a 0.5 mm mesh, homogenized, and heat-treated in batches of 4–8 l (2 h at 121 °C/1 atm). This procedure does not entirely sterilize the sediment (possibly because the core of the batch does not reach the sterilization temperature/time within an autoclavation cycle), but kills off residual CB and maintains a sediment structure and/or composition amenable to CB growth. The heat-treated sediment was packed into eleven Plexiglas liners (inner diam. 4.3 cm, height, 10 cm, Fig. S1). The top layer of seven cores was inoculated with a few grams of a sediment enrichment culture of *Ca. Electronema* sp. GS [14]. These are in the following assigned as “CB-cores”. The microbial community in these cores was composed of a single cable bacterial strain, other bacteria present in the *Ca. Electronema* sp. GS enrichment, and bacteria which had survived heat treatment inside the sediment batch. To account for the contribution of the latter to the rates of N-transformation, four sediment cores were treated as above but not inoculated and served as control. These are in the following assigned as “CB-free cores”. The CB- and CB-free cores were then preincubated for 4 weeks in two separate aquaria with tap water, aerated with submerged air pumps, and held at 15 °C, to promote the growth of *Ca. Electronema* sp. GS in the CB-cores, as CB have been shown to grow faster in the presence of oxygen than under anoxic conditions with nitrate [11]. In freshwater sediment, that inherently hosts a low concentration of hydrogen sulfide, e-SOx relies on hydrogen sulfide derived from the acid-dissolution of FeS and recycled via the tight-coupling between e-SOx and sulfate reduction [17]. The water in both aquaria was replaced weekly to replenish nutrients. The development of an active *Ca. Electronema* sp. GS population was monitored through measurements of the EP distribution in the cores and through regular microscopic inspections of the sediment.

Following the preincubation period, three CB-cores were sampled for RNA extraction and served as oxalic controls. Then, both aquaria were sealed and the water purged with premixed N₂ and CO₂ (0.04%) gas to remove dissolved oxygen while maintaining constant pH. The oxygen concentration was <0.2% air saturation as monitored with fiber-optic O₂ sensors (FireStingO2, Pyroscience, Germany). A 1:1 mixture of K¹⁴NO₃ and K¹⁵NO₃ (¹⁵N-atom%: 98%; Sigma-Aldrich) was added to a final concentration of 200 μM. The nitrate concentration was kept constant by adding small aliquots from a 100 mM K¹⁴NO₃: K¹⁵NO₃ stock solution two to three times per week. After 2 days of exposure to anoxia and nitrate, the activity of the *Ca. Electronema* sp. GS population was assessed through measurements of the EP distribution in the CB-cores. After 3 days of exposure, N-fluxes at the sediment-water interface were measured over a period of 10 days to assess the rates of nitrate reduction in the CB- and the CB-free cores. Thereafter, sediment samples for RNA analysis were collected from the CB-cores.

The EP distribution and e-SOx activity

The activity of the *Ca. Electronema* sp. GS. population during the preincubation period and during nitrate exposure was inferred from the depth distribution of the EP as described previously [12]. Depth distribution of the EP was measured with a customized EP microelectrode [18] against a Red Rod reference electrode (REF201 Radiometer Analytical, Denmark) kept in the overlying water (Fig. S1). Both electrodes were connected to an in-house-made milli-voltmeter with a resistance >10¹⁴ Ω (Aarhus University, Denmark). The analog signal from the milli-voltmeter was digitized for PC-processing using a 16-bit A/D converter (ADC-216; Unisense A/S, Denmark). To control its stepwise movement, the micro-electrode was fixed to a 1D microprofiling system (Unisense A/S, Denmark). The software Sensor Trace PRO was used to control the movements of the sensor and for logging the sensor signals. During the preincubation period, the EP-distribution was measured four times in the CB- and twice in the CB-free cores to evaluate the establishment (or lack) of e-SOx activity.

During the nitrate exposure period, the EP-distribution was measured only in the CB-cores to quantify the overall e-SOx activity of the *Ca. Electronema* sp. GS population and its ability to perform cathodic nitrate reduction. For this, cores were removed from the aquarium and fitted with a top Plexiglass tube (Fig. S1) that allowed to maintain an overlying water column of 150 mL. The tube was filled with nitrate-free water kept aerated

(100% air saturation) and gently stirred with an air pump. CB activity was tested by sediment EP microprofiling as described above. Successively, to evaluate the magnitude of the “residual” EP (i.e., not due to e-SOx activity), EP profiling was repeated after oxygen was removed from the water by gentle purging with premixed N₂ and CO₂ (0.04%) gas. Finally, to test the ability of *Ca. Electronema* sp. GS to perform cathodic nitrate reduction, EP profiling was conducted after the addition of a concentrated (10 mM) KNO₃ anoxic solution to the water (final conc.: 200 μM). The magnitude of the electron flux *J* was calculated for the CB-cores exposed to oxalic or anoxic water with nitrate according to [12]:

$$J = \left| -\sigma \left(\frac{d\psi_{+e \text{ acceptor}}}{dz} - \frac{d\psi_{-e \text{ acceptor}}}{dz} \right) \right| \frac{1}{F} \quad (1)$$

Where $d\psi_{+e \text{ acceptor}}/dz$ is the linear gradient of the EP in the oxygen or nitrate zone measured in the presence of either of the two electron acceptors in the water column. $d\psi_{-e \text{ acceptor}}/dz$ is the gradient of EP in the same zone measured in the absence of electron acceptors. *F* is the Faraday's constant and σ is the sediment conductivity estimated from the conductivity of the sediment porewater and the porosity, according to [19]. The conductivity of the porewater was measured with a conductivity meter (Mettler Toledo, Fisher Scientific, USA).

¹⁵N-based quantification of nitrate reduction pathways

The CB- and the CB-free cores in the ¹⁵NNO₃-amended aquaria were equipped with top Plexiglas tubes (Fig. S1). The water enclosed in the tubes (~150 ml) was kept mixed by the Teflon-coated magnetic stir bar suspended at a few centimeters above the sediment and driven by an external rotating magnet. The sediment cores with mounted tubes were maintained submerged inside the anoxic aquarium with the lids open and the stirrers on, to assure initial homogenous conditions. Prior to the start of the incubation, water samples for analysis of nitrite, ammonium, and di-nitrogen total concentration and isotopic composition were collected from the aquaria with a syringe. Samples for nitrite and ammonium analysis were transferred to plastic vials, immediately placed on ice, and subsequently frozen (−20 °C) until further analysis. Samples for di-nitrogen analysis were transferred into 12 ml Exetainers (Labco, U.K.) and fixed with 250 μL ZnCl₂ (50:50 w/v). The tubes were then sealed with lids to initiate the incubation. After a 3- to 4-h incubation period, the lids were removed and the water was sampled for nitrite, ammonium, and di-nitrogen total concentration and isotopic composition as described above. At the end of the sampling procedure, the cores were placed back in the anoxic aquarium for 1 to 3 days with the lid open before the incubation was repeated. The incubation procedure was repeated three times over the span of 10 days to confirm the stability of the system, thereby confirming that reaction rates can be approximated to the fluxes. Fluxes of N-isotopologues were calculated according to: $J = (C_{\text{end}} - C_{\text{start}})/(A \times t)$, where *C*_{end} and *C*_{start} are the concentrations of a given N-species in the overlying water at the end and at the start of the incubation, respectively; *A* is the surface area of the sediment core; and *t* is the incubation time. Rates of DNRA were calculated from the ¹⁵NNH₄⁺ flux divided by the fraction of [¹⁵NO₃[−]] to total [NO₃[−]] in the aquaria, i.e., 0.45. Rates of NH₄⁺ production from organic matter mineralization were calculated from total NH₄⁺ fluxes (i.e., ¹⁴+¹⁵N) – rates of DNRA. Rates of denitrification were calculated from the fluxes of ²⁹N₂ and ³⁰N₂ according to [20]. Rates of nitrite production were estimated from the fluxes of nitrite. The isotopic composition of di-nitrogen and ammonium was determined by mass spectrometry on a 20-22 hydra Isotope Ratio Mass Spectrometer (SerCon, Crewe, U.K.). [²⁹N₂] and [³⁰N₂] were determined as described in [21], while the ¹⁵N-atom% of ammonium was determined with the Combined Microdiffusion-Hypobromite Oxidation Method [22]. [¹⁵NH₄⁺] was calculated as the product of the ¹⁵N-atom% of ammonium and the ammonium concentration, the latter being determined with the Salicylate-Hypochlorite Method [23]. Nitrite concentrations were determined by ion chromatography (Dionex IC-2500, Thermo Fisher Scientific).

RNA sampling and extraction

Three CB-cores were sampled after the preincubation period (oxic controls) and three CB-cores were sampled after the anoxic ¹⁵NNO₃[−] amended incubation. Sediment cores were extruded from the liners using a threaded rod. The upper 1 mm section from each core was transferred to 10 mL Falcon tubes and snap-frozen into liquid nitrogen. Total RNA from each sediment sample was extracted using the RNeasy PowerSoil Total RNA Kit (Qiagen). The RNA was concentrated with the kit RNA Clean &

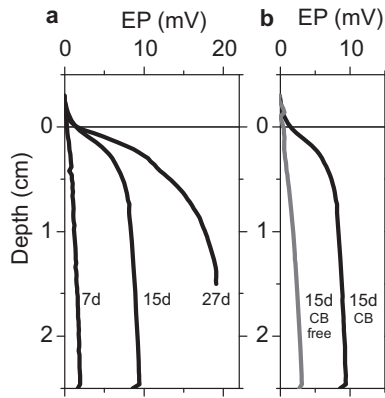


Fig. 1 Development of electric potential in sediment cores. Electric potential (EP) depth profiles in sediment cores at days 7, 15, and 27 after the inoculation with cable bacteria (CB) (panel a). EP depth profiles in a sediment core at day 15 after the inoculation with cable bacteria (black line) and a CB-free core not inoculated (gray line) (panel b). Data are shown as mean ($n = 3$).

Concentrator (Zymo Research, USA) with an in-column DNase treatment (Ambion, USA) and stored at -80°C before sequencing. High-throughput sequencing (HiSeq, SR50 reads, Illumina, USA) was performed by DNASense (Aalborg, Denmark), after 16 S and 23 S rRNA removal with the Ribo-Zero rRNA Removal Kit for Bacteria (Illumina, USA).

Transcriptomic analysis

Metatranscriptome reads ($\sim 7 \times 10^7$ per sample) were mapped onto the genome of *Ca. Electronema sp. GS* [14] using the IMG annotation (taxon id 2728369268) and standard parameters in the software Seal (<https://jgi.doe.gov/data-and-tools/bbtools/bb-tools-user-guide/seal-guide/>). The mapped reads were normalized to gene length and total read depth using the method reads per kilobase transcript per million mapped reads (RPKM) and ranked to determine the uniform expression levels. Differential expression between the nitrate incubations and the oxic controls was tested with the DESeq2 R package [24], with the false discovery rate (FDR) adjusted to 0.1. The analysis focused on *Ca. Electronema sp. GS* genes presumably involved in nitrate and nitrite reduction (*napA* and gene neighborhood) as proposed in [14]. In addition, the metatranscriptome reads were assembled with rnaSPAdes (v. 3.14) [25] and annotated with FragGeneScan (v.1.31) [26]. The annotated amino acid sequences were scanned for *nrfA*, *nirK*, and *nirS* with *hmmsearch* (v.3.1b2) and *hmm* matrices from the FunGene repository [27]. Then the metatranscriptome reads were mapped to the identified *nrfA*, *nirK*, and *nirS* transcript fragments in Seal using standard parameters. Transcriptomic data are available at NCBI/SRA under accession numbers PRJNA575156 and PRJNA575166.

Phylogenetic analysis

Published *nrfA* [28] and *napA* [29] phylogenies were used to retrieve reference sequences for phylogenetic analyses of pOCC and *napA*, together with closest BLAST hits and, for pOCC, characterized, highly similar proteins from *Beggiatoa* [16] and Epsilonproteobacteria (*eHao*) [30] (Table S1 and S2). Reference sequences for *napD* and *napF* phylogenetic analysis were selected from the same genomes as *napA* when present (Table S3 and S4). *napA*, *nrfA/eHao/pOCC*, *napD*, and *napF* were translated in silico, and amino acid sequences were aligned using the Muscle algorithm in Mega X version 10.0.5 with standard settings. Phylogenies were reconstructed using the maximum-likelihood algorithm in Mega X version 10.0.5 with a model of rate heterogeneity and the LG+G (NapA, NapD, and NapF) or WAG+G (pOCC) protein substitution model. The node stability was tested by bootstrapping (1000 resamplings).

RESULTS

The EP distribution in CB- and CB-free cores during preincubation

During the oxic preincubation, the EP at 1.5 cm depth increased progressively in the CB-cores to a maximum of 20 mV after

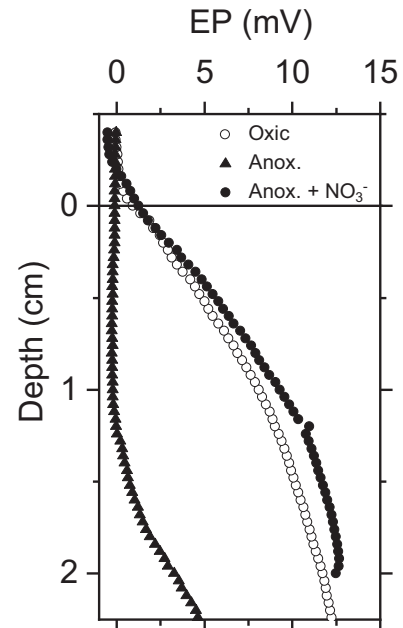


Fig. 2 Electric potential under oxic, anoxic and nitrate-amended conditions. EP depth profiles in a CB-core sequentially exposed to aerated (white circles), anoxic, nitrate-free (black triangles), and anoxic nitrate-amended (black circles) water. Data are shown as mean ($n = 3$).

27 days (Fig. 1a). The magnitude of the electric field estimated from the gradient of the EP in the oxic zone (top 1 mm. Gradient calculated in the 0.2 to 1.5 mm depth interval) increased from 0.18 to 1.8 V m^{-1} at week 2 and to 3.5 V m^{-1} at week 4. This progressive increase in field strength confirmed that *Ca. Electronema sp. GS* was growing in the CB-cores. The EP was measured in the CB-free cores after 2 weeks of preincubation and reached 2.4 mV at 1.5 cm depth (Fig. 1b). The magnitude of the electric field in the 0.2–1.5 mm depth interval was 0.03 V m^{-1} , corresponding to 2.5% of the field strength in the CB-cores. This low field strength was taken as evidence for the insignificant presence of CB- in the CB-free cores, a pattern that was confirmed from microscope inspection prior to moving the cores into the anoxic, nitrate-amended aquaria.

Electron acceptor switch experiment with CB-cores

The EP distribution measured in CB-cores incubated for 2 days in anoxic, nitrate-amended water is shown in Fig. 2. When the CB-core was exposed to air-saturated, nitrate-free water, the EP at 1 cm depth was 8 mV and the electric field in the 0–1.5 mm domain was 0.95 V m^{-1} or 27% of the field strength measured prior to the transfer, indicating a drop in CB activity. When the water above the sediment was turned anoxic, the EP at 1 cm depth and the electric field in the 0.2–1.5 mm domain was close to zero. When $200 \mu\text{M}$ nitrate was added to the anoxic water overlying the sediment, the EP at 1 cm depth and the electric field in the nitrate reduction zone (i.e., 0 to <1.5 mm depth. Gradient calculated in the 1.2–2.4 mm depth interval) was similar to those measured in the presence of an oxygen saturated, nitrate-free water column, i.e., 10 mV and 1.0 V m^{-1} , respectively. These observations suggest that the population of *Ca. Electronema sp. GS* was active both in the presence of oxygen saturated, nitrate-free water column and in the presence of an anoxic nitrate-amended water column, but also that the activity of the population had declined significantly after being exposed to anoxia and nitrate for 2 days (electric field at the end of the oxic preincubation = 3.5 V m^{-1} , see above and Fig. 1). The electron flux estimated from the EP profile measured in the presence of nitrate was $1.3 \pm 0.1 \text{ mmol e}^{-} \text{ m}^{-2} \text{ h}^{-1}$ (mean \pm s.e.m., $n = 3$).

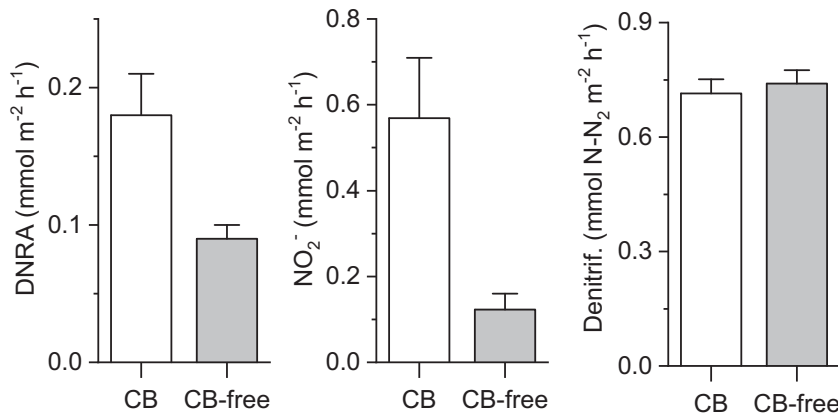


Fig. 3 Rates of DNRA, nitrite production and denitrification. Net fluxes of NO_2^- , N_2 from denitrification (D_w), and NH_4^+ from DNRA (i.e., from water column NO_3^- reduction) across the sediment-water interface during anoxic incubations of sediment inoculated with cable bacteria (CB) and in control (CB-free) cores. Data were shown as mean \pm s.e.m. ($n = 12$).

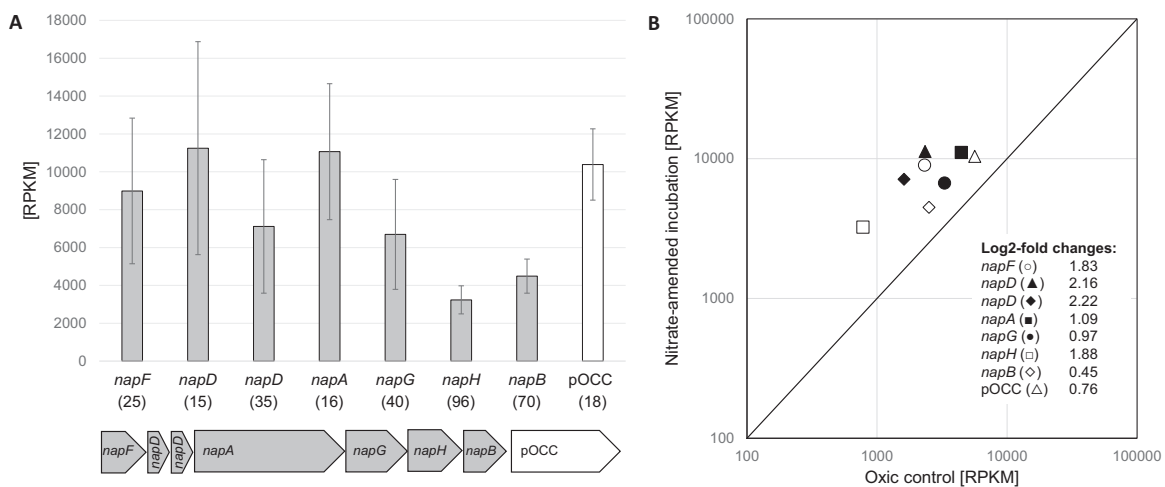


Fig. 4 Structure and gene expression of the putative DNRA genes in *Ca. Electronema* sp. GS. **A** Operon structure and expression levels under nitrate-reducing conditions ($n = 3$, \pm s.e.m.). The rank of each gene in the transcriptome is shown in parenthesis. RPKM reads per kilobase per million. **B** Expression of the *nap*-pOCC operon after nitrate-amendment compared to the oxic controls ($n = 3$).

¹⁵N-based quantification of the nitrate reduction pathways

Rates of DNRA measured in the CB-cores were significantly different from those measured in the CB-free cores (t -test, $p = 0.007$, $n = 24$) and up to twofold higher (Fig. 3). Rates of nitrite production in the CB-cores were significantly different from those measured in the CB-free cores (t -test, $p = 0.008$, $n = 24$) and up to fivefold higher. There was no significant difference in denitrification rates between CB- and CB-free cores (t -test, $p = 0.26$, $n = 24$). Rates of NH_4^+ production from organic matter mineralization (i.e., $^{14+15}\text{NH}_4^+$ - DNRA) did not differ between CB- and CB-free cores (t -test, $p = 0.61$, $n = 24$. CB cores = $0.83 \pm 0.06 \mu\text{mol m}^{-2} \text{h}^{-1}$; CB-free cores = $0.86 \pm 0.03 \mu\text{mol m}^{-2} \text{h}^{-1}$).

Operon structure and expression of genes putatively involved in nitrate and nitrite reduction

Detailed analysis of the gene neighborhood of the *napAB* genes revealed that *Ca. Electronema* sp. GS contained a complete *nap* operon encoding all components for periplasmic reduction of nitrate to nitrite (Fig. 4): the maturation factor NapF, two copies of the chaperone NapD, the electron-transferring membrane complex NapGH, and the catalytic complex NapAB. The gene encoding the pOCC, was located directly downstream of the *nap* operon (Fig. 4A). This pOCC contains a signal peptide and no transmembrane helices. All eight genes were among the 100 most highly

expressed genes (out of 2649 total genes) under nitrate-reducing conditions (Fig. 4 and Table S5). A comparison of gene expression levels between the nitrate-amended incubations and the oxic controls showed that all eight consecutive genes were slightly but consistently upregulated under nitrate-reducing conditions (Fig. 4B). However, according to DESeq2 analysis, none of these upregulations were statistically significant (Table S5).

Scanning the assembled metatranscriptome for non-CB nitrite reductase transcripts, indicative of other active nitrite-reducing microbial community members, identified 16 *nirK*, 63 *nirS*, and 40 *nrfA* transcript fragments, with a total number of 3689, 89,639, and 11,536 reads mapping to these fragments, respectively (Table S6–8). In comparison, 21,010 reads mapped to the pOCC of *Ca. Electronema* sp. GS.

Phylogeny of the putative nitrate reduction system

BLAST searches against the NCBI database retrieved closest matches for *napF* (44.9% translated amino acid identity), *napD* (50.6 and 43.2%), and pOCC (73.8%) to homologs in the marine cable bacterium *Ca. Electrothrix aarhusiensis* MCF [14], and additional matches for pOCC (70.0%) and *napF* (53.1%) to gene fragments in the less complete genomes of *Ca. Electrothrix marina* A3 and A5, respectively. No other *nap* genes were at first detected in these marine CB, i.e., the *nap* operon appeared incomplete.

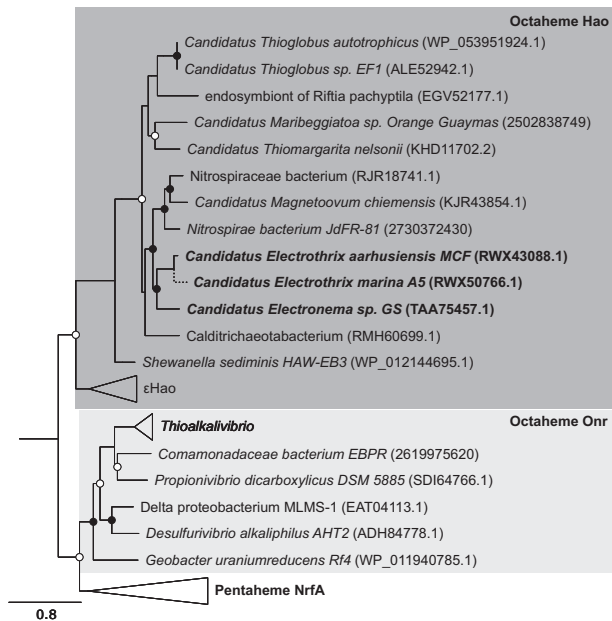


Fig. 5 Phylogenetic affiliation of cable bacterial putative octaheme cytochromes (pOCC) with ϵ Hao and the pentaheme NrfA proteins. Consensus tree by maximum likelihood with 1000 bootstrap resamplings. Bootstrap values are represented by circles: open >70%, filled >90%. Tree was rooted with the nitrite reductase (NirB) of *Bacillus subtilis*. Scale bar represents 0.8 estimated amino acid substitutions. The phylogenetic position of the short NapF fragment of *Ca. E. marina* was calculated by the maximum parsimony method in the program ARB [54] without changing the overall tree topology. For an expanded phylogenetic tree, see Fig. S4.

However, a closer inspection of the *Ca. E. aarhusiensis* MCF genome revealed that *napF* is located at the end of a contig, and a truncated *napA* fragment is located at the end of another (short) contig. This fragmentation suggests that the rest of the *nap* operon was missed during sequencing/genome assembly in *Ca. E. aarhusiensis* MCF. Phylogenetic analysis placed the cable bacterial NapA-, NapD-, and NapF-lineages in clades containing different alpha-, beta-, or gammaproteobacterial genes (Figs. S2, S3, and S4). The cable bacterial pOCC formed a monophyletic clade with homologs from sediment-dwelling bacteria of at least three phyla (Nitrospirae, Caldritrichaeota, and Gammaproteobacteria, which include large sulfur bacteria; Figs. 5 and S5). This pOCC clade furthermore forms a sister clade to members of the epsilonproteobacterial hydroxylamine oxidoreductase (ϵ Hao) family [30], which together branch off from the canonical pentaheme nitrite reductases (NrfA) and octaheme nitrite reductases (Onr) [31].

DISCUSSION

Nitrate reduction associated with *Ca. Electronema sp. GS*

The higher rates of nitrite production in the CB cores as compared to the CB-free cores, and the presence of transcripts from a CB affiliated *nap* operon, that encoded all components needed for periplasmic reduction of nitrate to nitrite, indicates that *Ca. Electronema sp. GS* actively reduced nitrate to nitrite in the CB cores. Previous results suggest that CB did not only reduce nitrate but also possess the ability to reduce the nitrite further [12]. We can exclude the possibility that *Ca. Electronema sp. GS* reduced nitrite to N_2 as results from the ^{15}N experiment showed similar rates of N_2 production in CB- and CB-free cores thereby suggesting that denitrification has to be attributed to a denitrifying community inherently present in the sediment prior

to the inoculation with CB (i.e., linked with microbial strains that have survived heat treatment as indicated by a large number of non-CB *nirK* and *nirS* transcripts in the metatranscriptome (Table S6). The lack of increased N_2 production in cores inoculated with *Ca. Electronema sp. GS* is aligned with previous studies on marine CB showing no electric field development in response to N_2O additions [12].

The higher rates of DNRA in CB-cores compared to CB-free cores indicate that *Ca. Electronema sp. GS* favors DNRA activity. As mentioned above, this can be the direct result of its metabolism or an indirect effect of e-SOX [13]. The overall nitrate reduction activity that can be attributed to *Ca. Electronema sp. GS* can be estimated from the difference in rates between CB and CB-free cores. For NO_2^- production (i.e., the reduction of NO_3^- to NO_2^-) this amounts to $446 \pm 73 \mu mol NO_2^- m^{-2} h^{-1}$ (mean + s.e.m, $n = 24$), whereas $89.7 \pm 16 \mu mol NH_4^+ m^{-2} h^{-1}$ were produced from DNRA. As the reduction of NO_3^- to NO_2^- requires 2 moles of electrons per mole of NO_3^- and the reduction of NO_3^- to NH_4^+ requires 8 moles of electrons per mole of NO_3^- , the overall electron demand of the nitrate reduction activity attributed to the presence of *Ca. Electronema sp. GS* is $(0.446 \times 2) + (0.089 \times 8) = 1.61 \pm 0.1 mmol e^- m^{-2} h^{-1}$ (mean + s.e.m, $n = 48$; 95% Confidence Interval [1.41–1.81]). The flux of electrons supplied from the anodic oxidation of sulfide by *Ca. Electronema sp. GS*, estimated from the EP profiles in Fig. 2, amounted to $1.27 \pm 0.06 mmol e^- m^{-2} h^{-1}$ (mean \pm s.e.m. $n = 3$; 95% CI: 1.03–1.51). Although this flux seems to be in the lower end of what is needed to drive the estimated rates of nitrate and nitrite reduction, the hypothesis that the electron flux from e-SOX by *Ca. Electronema sp. GS* is equal to the electron demand for nitrate reduction to nitrite and DNRA cannot be rejected for $\alpha = 0.05$. As previous studies showed that CB can reduce nitrite [12], we suggest that the elevated rates of DNRA observed in the CB cores are directly associated with the nitrate reduction capacity of *Ca. Electronema sp. GS*. The accumulation of nitrite observed in our experiment could be linked to the differences in kinetic properties and concentrations of the enzymes involved in the respective reduction processes (e.g., [32]). It has to be noted, however, that the variability associated with our measurements prevents us to rule out a possible contribution of the indirect stimulation of Fe^{2+}/H_2S driven-DNRA as proposed by Kessler et al. [13].

The capability of *Ca. Electronema sp. GS* to reduce nitrate to nitrite is in line with the presence and expression of a complete *nap* operon (Fig. 4A), where the only unusual feature appears to be a duplication of the chaperone-encoding *napD* [33]. Thus, our data indicate that nitrate reduction occurs in the periplasm by the NapAB system. In contrast, identification of the enzyme responsible for nitrite reduction to ammonium is more challenging, and our suggestion of the pOCC as nitrite reductase remains uncertain with the current data. On one hand, the sequential *nap*-pOCC gene structure (Fig. 4A) is syntenic to that of the well-characterized nitrate and nitrite-reducing genes of epsilonproteobacteria [30], suggesting a linked function of Nap and pOCC for DNRA; the pOCC is, together with the entire *nap* operon, highly expressed under nitrate-reducing conditions (Fig. 4A, B and Table S5) and shows much higher expression than the few non-CB *nrfA* fragments detected in the metatranscriptome (Table S6); furthermore the pOCC features the eight heme-binding sites conserved among nitrite-reducing pOCCs (Fig. S6), e.g., of the ϵ Hao clade (Fig. 5) [30], and contains a conserved tryptophan residue implicated in a reducing function in Hao [30] (Fig. S6). On the other hand, the octaheme cytochrome c family, although descended from the nitrite-reducing NrfA pentahemes [31], contains both nitrite reductases, hydroxylamine oxidoreductases, and tetrathionate reductases [30, 31], and the activity of these enzymes cannot be unambiguously predicted from their amino acid sequences [30, 31]. Therefore, although some indications suggest the pOCC as a candidate for an ammonium-producing

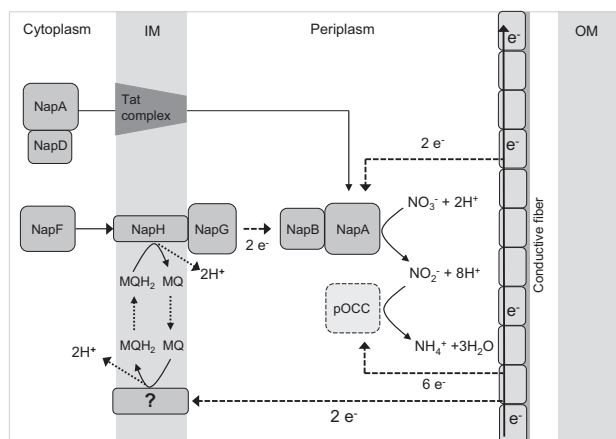


Fig. 6 Model of cathodic nitrate reduction to ammonium in *Ca. Electronema sp. GS*. Dotted arrows indicate electron flows. Electrons are derived from anodic sulfide oxidation and delivered via the periplasmic conductive fiber to the periplasmic NapAB complex that mediates nitrate reduction to nitrite and to pOCC that putatively mediate nitrite reduction to ammonium. Electron flow could occur merely in the periplasm or involve menaquinone cycling and the membrane-bound NapHG complex.

nitrite reductase in CB, ultimately the purification and characterization of the protein is needed to determine its function.

Origin and distribution of dissimilatory nitrate reduction in CB

Cable bacteria, including *Ca. Electronema sp. GS*, are a monophyletic sister group to the genus *Desulfobulbus* within the deltaproteobacterial Desulfobulbaceae. In contrast, none of their *nap* and *pOCC* genes were phylogenetically affiliated with deltaproteobacterial genes (Fig. 5 and Figs. S2–S5). This indicates that all genes for nitrate and (putative) nitrite reduction have been acquired by horizontal gene transfer, and since the various genes show distinct evolutionary histories, probably in multiple events from different organisms. Possible donors for the different *nap* genes are different members of the Alpha-, Beta-, and Gamma-proteobacteria (Figs. S2–4). For the *pOCC*, it is intriguing that the most closely related genes were from bacteria that can co-occur with CB in sulfide-oxygen gradients of surface sediments, like the large sulfur bacteria *Thiomargarita* or *Beggiatoa* [9, 34], *Calditrichaota* [35], or the magnetotactic bacterium *Magnetoovum* [36]. This implies that horizontal gene transfer may occur between such phylogenetically distant organisms in this shared niche.

It is currently difficult to infer how widespread the capability to reduce nitrate and nitrite is among CB on the sole basis of genomic evidence. The only complete putative DNRA pathway was detected in our model freshwater species *Ca. Electronema sp. GS* (Fig. 4), while the same genes were rare and fragmented in the other five CB genomes available which belong to the marine genus *Ca. Electrothrix* [14]. The observation of nitrite- and possibly nitrate-dependent e-SOx in marine sediment [11, 12], indicates, however, that the lack of complete nitrate/nitrite reducing genes in *Ca. Electrothrix* can be, at least for the targeted species, attributed to incomplete and highly fragmented genomes (see results above and [14]). Future efforts in compiling CB genomes will provide insights on the potential for nitrate and nitrite reduction in different CB species. It is however striking that the genes detected in *Ca. Electrothrix* (*napF*, *napD*, and *pOCC*) always cluster with their freshwater homolog in *Ca. Electronema sp. GS* (Fig. 5 and Figs. S2–5). As crossovers between freshwater and marine species are rare [37], this indicates that the capacity for nitrate/nitrite reduction was acquired by CB before their diversification into different salinity niches represented by the candidate genera *Electrothrix* and *Electronema* [38, 39]. This

scenario suggests that all CB originally were capable of nitrate/nitrite reduction, but the pathway (or part of it) may subsequently have been lost in certain species or lineages, as is commonly observed for canonical nitrate reducers and denitrifiers [40–42].

Hypothetic model of the nitrate reduction system of *Ca. Electronema*

On the basis of the transcriptome data and the morphology of CB a model of the architecture of the nitrate reduction system in *Ca. Electronema sp. GS* can be hypothesized (Fig. 6). *Ca. Electronema sp. GS* transcribed a complete *napFDDAGHB* operon, as well as genes encoding a putatively nitrite-reducing pOCC. The general arrangement and biochemical role of the proteins produced from the *napFDDAGHB* transcripts can be drafted from the model of the respiratory Nap system of the epsilonproteobacterium *Wolinella succinogenes* [33, 43]. According to this model, the nitrate-reducing NapAB complex is located in the inner membrane. The NapGH complex is embedded in the inner membrane and catalyzes the oxidation of reduced menaquinones dissolved in the inner membrane, passing the electrons to NapA via NapB. According to Simon and Klotz [33], the NapGH complex transfers the protons liberated from menaquinone oxidation to the periplasm. The NapD is a chaperone protein that assists the transfer of mature NapA via the TAT complex (also present and expressed in *Ca. Electronema sp. GS*, data not shown) from the cytoplasm to the periplasm, whereas the NapF protein, located in the cytoplasm is proposed to provide reducing power for the maturation of NapA [33]. In *W. succinogenes*, nitrate reduction via the Nap system involves the reduction of menaquinones by a membrane-bound formate dehydrogenase (FdhABC) [43], and a proton motive force (pmf) is supposedly generated through the NapGH-FdhABC mediated redox cycle of the menaquinones [43]. If the Nap system of *Ca. Electronema sp. GS* should work in a similar way, but driven by e-SOx, electrons for menaquinone reduction should be delivered from the conducting strings present in the periplasm [2] via, e.g., the highly expressed periplasmic cytochromes [14, 44] and a hitherto unidentified membrane-bound menaquinone reductase (like, e.g., the Type I cytochrome c3:menaquinone oxidoreductase protein Qrc found in *Desulfovibrio vulgaris* Hildenborough [45]). E-SOx-mediated nitrate reduction via the conventional Nap pathway would further imply electron transport from anodic cells to cathodic cells both having electron carrier molecules with identical standard redox potential, as menaquinones are also implicated in cytoplasmic redox cycling during anodic sulfide oxidation in *Ca. Electronema sp. GS* [14]. Modeling such transport from a concentration cell analog (Fig. S7 - Extended discussion) shows that such an electron flow is thermodynamically feasible (i.e., $E > 0V$) as long as a larger fraction of the menaquinone pool is kept oxidized in the cathodic compared to the anodic cells, and that the voltage produced by a 2 cm long filament can be sufficiently high to drive an electric current (>1 nA) that exceeds the current reported in the literature for CB (i.e., 0.2–0.36 nA [4, 7, 46]).

The putative nitrite reductase (pOCC) of *Ca. Electronema sp. GS* has presumably a periplasmic localization with no membrane anchor, as also suggested for its close homolog in *Ca. Maribeggiatoa sp.* [15]. From the genome data, we cannot identify an electron donor that links nitrite reduction to menaquinone cycling, as homologs to, e.g., the NrfHA system in Epsilonproteobacteria [47], the NrfBCD system in Gammaproteobacteria [33], and the CymA system in *Shewanella oneidensis* [48, 49] are absent in CB. It is possible that nitrite reduction in *Ca. Electronema sp. GS* is fully periplasmic and decoupled from menaquinone cycling. In this scenario, the pOCC would receive electrons directly from the conducting strings or via other periplasmic cytochromes.

In *W. succinogenes*, proton production from FdhABC-mediated formate oxidation matches the proton consumption

from periplasmic nitrate reduction [43]. NapGH-mediated proton transfer into the periplasm could therefore in principle produce a pmf, which could drive ATP synthesis through oxidative phosphorylation. The generation of a pmf by NapGH in *Ca. Electronema* sp. GS is however less likely, as protons from electron donor oxidation are produced by distant anodic cells in the filament [1, 3], implying proton deficiency in the periplasm of the nitrate-reducing cathodic cells and consequently loss of pmf through proton consumption by periplasmic nitrate reduction. Alternative electron flows, such as direct electron transfer from the conductive strings via periplasmic cytochromes to the NapAB complex or to pOCC would not generate a pmf during nitrate/nitrite reduction either, as these enzyme-mediated reactions take place in the periplasm, disconnected from the cytoplasmic membrane. In conclusion, cathodic cells performing nitrate reduction cannot conserve energy through oxidative phosphorylation. This matches the situation proposed for oxygen-reducing cathodic CB cells, which appear to perform periplasmic oxygen reduction without energy conservation [14, 50, 51].

Conclusions and perspectives

Our geo-electro-chemical and transcriptomic evidences indicate that *Ca. Electronema* sp. GS reduces nitrate to nitrite by a NapAB complex. Moreover, our data suggest the ability of *Ca. Electronema* sp. GS to further reduce nitrite to ammonium possibly by pOCC, although the function of pOCC in CB remains to be characterized. The capability for nitrate and nitrite reduction has likely been acquired by horizontal gene transfer from phylogenetically distant organisms that share the same ecological niche.

The periplasmic allocation of NapAB and pOCC implies no energy conservation via oxidative phosphorylation in association with nitrate/nitrite reduction, supporting the hypothesis of a division of labor along the CB filament, with the cathodic cells serving primarily as “flare” for electrons delivered by the anodic cells. In this scenario, high energy-demanding transcription and protein synthesis occur primarily in the suboxic zone [14, 50, 51], and the movement of CB filaments [52] across the sediment geochemical gradient alternates the exposure of CB cells to sulfide-oxidizing and nitrate-reducing conditions; the limited ATP demand for protein repair (e.g., by chaperones) and maintenance in the cathodic cells may be provided from storage compounds (polyphosphate, polyglucose [14]) produced under anoxic conditions. The apparent duplication of the chaperon napD (Fig. 4) may be an adaptation to this lifestyle.

From a geochemical perspective, our incubations showed that the presence of CB doubles the rate of DNRA, thereby increasing the relative importance of fixed nitrogen recycling over its removal via denitrification. As we applied sediment hosting a simplified bacterial community, the fate of the CB-produced ammonium (and nitrite) in a more complex natural community and consequently the overall impact of e-SOx on the benthic nitrogen cycle cannot be fully constrained. CB have also been reported to stimulate DNRA activity indirectly in riverine sediment incubated under laboratory conditions, by promoting the activity of Fe²⁺ and/or H₂S chemolithotrophs [13]. As both studies converge in showing increased DNRA linked with e-SOx, and given their global distribution [5, 53], CB could potentially play a so far overlooked role in regulating the balance between denitrification and DNRA in benthic systems. This might be particularly relevant in eutrophic freshwater environments characterized by high nitrate concentrations and transient to permanent anoxic conditions. In situ occurrence, regulation, and relevance of e-SOx driven DNRA remains to be evaluated.

REFERENCES

- Pfeffer C, Larsen S, Song J, Dong M, Besenbacher F, Meyer RL, et al. Filamentous bacteria transport electrons over centimetre distances. *Nature*. 2012; 491:218–21.
- Meysman FJR, Cornelissen R, Trashin S, Bonn e R, Martinez SH, van der Veen J, et al. A highly conductive fibre network enables centimetre-scale electron transport in multicellular cable bacteria. *Nat Commun*. 2019;10:4120.
- Nielsen LP, Risgaard-Petersen N, Fossing H, Christensen PB, Sayama M. Electric currents couple spatially separated biogeochemical processes in marine sediment. *Nature*. 2010;463:1071–4.
- Malkin SY, Rao AM, Seitaj D, Vasquez-Cardenas D, Zetsche EM, Hidalgo-Martinez S, et al. Natural occurrence of microbial sulphur oxidation by long-range electron transport in the seafloor. *ISME J*. 2014;8:1843–54.
- Burdorf LDW, Trampler A, Seitaj D, Meire L, Hidalgo-Martinez S, Zetsche EM, et al. Long-distance electron transport occurs globally in marine sediments. *Biogeochemistry*. 2017;14:683–701.
- Marzocchi U, Bonaglia S, van de Velde S, Hall POJ, Schramm A, Risgaard-Petersen N, et al. Transient bottom water oxygenation creates a niche for cable bacteria in long-term anoxic sediments of the Eastern Gotland Basin. *Environ Microbiol*. 2018;20:3031–41.
- Risgaard-Petersen N, Kristiansen M, Frederiksen RB, Dittmer AL, Bjerg JT, Trojan D, et al. Cable bacteria in freshwater sediments. *Appl Environ Microbiol*. 2015;81:6003–11.
- Risgaard-Petersen N, Revil A, Meister P, Nielsen LP. Sulfur, iron-, and calcium cycling associated with natural electric currents running through marine sediment. *Geochim Cosmochim Acta*. 2012;92:1–13.
- Seitaj D, Schauer R, Sulu-Gambari F, Hidalgo-Martinez S, Malkin SY, Burdorf LD, et al. Cable bacteria generate a firewall against euxinia in seasonally hypoxic basins. *Proc Natl Acad Sci USA*. 2015;112:13278–83.
- Sulu-Gambari F, Seitaj D, Meysman FJR, Schauer R, Polerecky L, Slomp CP. Cable bacteria control iron–phosphorus dynamics in sediments of a coastal hypoxic basin. *Environ Sci Technol*. 2016;50:1227–33.
- Marzocchi U, Trojan D, Larsen S, Meyer RL, Revsbech NP, Schramm A, et al. Electric coupling between distant nitrate reduction and sulfide oxidation in marine sediment. *ISME J*. 2014;8:1682–90.
- Risgaard-Petersen N, Damgaard LR, Revil A, Nielsen LP. Mapping electron sources and sinks in a marine biogeochemical battery. *J Geophys Res Biogeosci*. 2014; 119:1475–86.
- Kessler AJ, Wawryk M, Marzocchi U, Roberts KL, Wong WW, Risgaard-Petersen N, et al. Cable bacteria promote DNRA through iron sulfide dissolution. *Limnol Oceanogr*. 2018;64:1228–38.
- Kjeldsen KU, Schreiber L, Thorup CA, Boesen T, Bjerg JT, Yang T, et al. On the evolution and physiology of cable bacteria. *Proc Natl Acad Sci USA*. 2019;116:19116–25.
- MacGregor BJ, Biddle JF, Siebert JR, Staunton E, Hegg EL, Matthyse AG, et al. Why orange Guaymas Basin Beggiatoa spp. are orange: single-filament-genome-enabled identification of an abundant octaheme cytochrome with hydroxylamine oxidase, hydrazine oxidase, and nitrite reductase activities. *Appl Environ Microbiol*. 2013;79:1183–90.
- Buckley A, MacGregor B, Teske A. Identification, expression and activity of candidate nitrite reductases from orange Beggiatoaceae, Guaymas Basin. *Front Microbiol*. 2019;10:644.
- Sandfeld T, Marzocchi U, Petro C, Schramm A, Risgaard-Petersen N. Electrogenic sulfide oxidation mediated by cable bacteria stimulates sulfate reduction in freshwater sediments. *ISME J*. 2020;14:1233–46.
- Damgaard LR, Risgaard-Petersen N, Nielsen LP. Electric potential microelectrode for studies of electrobiogeophysics. *J Geophys Res Biogeosci*. 2014;119:1906–17.
- Archie GE. The electrical resistivity log as an aid in determining some reservoir characteristics. *T Am I Min Met Eng*. 1942;146:54–61.
- Nielsen LP. Denitrification in sediment determined from nitrogen isotope pairing. *Fems Microbiol Ecol*. 1992;86:357–62.
- Risgaard-Petersen N, Rysgaard S. Nitrate reduction in sediments and waterlogged soil measured by 15N techniques. In: Alef K, Nannipieri P, editors. *Methods in applied soil microbiology and biochemistry*. Academic Press; 1995. p. 287–95.
- Risgaard-Petersen N, Rysgaard S, Revsbech NP. Combined microdiffusion-hypobromite oxidation method for determining N-15 isotope in ammonium. *Soil Sci Soc Am J*. 1995;59:1077–80.
- Bower CE, Holmhansen T. A salicylate-hypochlorite method for determining ammonia in seawater. *Can J Fish Aquat Sci*. 1980;37:794–8.
- Love MI, Huber W, Anders S. Moderated estimation of fold change and dispersion for RNA-seq data with DESeq2. *Genome Biol*. 2014;15:550.
- Bushmanova E, Antipov D, Lapidus A, Pribelski AD. rnaSPAdes: a de novo transcriptome assembler and its application to RNA-Seq data. *Gigascience*. 2019; 8: giz100.

26. Rho M, Tang H, Ye Y. FragGeneScan: predicting genes in short and error-prone reads. *Nucleic Acids Res.* 2010;38:e191.
27. Fish JA, Chai B, Wang Q, Sun Y, Brown CT, Tiedje JM, et al. FunGene: the functional gene pipeline and repository. *Front Microbiol.* 2013;4:291.
28. Welsh A, Chee-Sanford JC, Connor LM, Löffler FE, Sanford RA. Refined *nrfA* phylogeny improves PCR-based *nrfA* gene detection. *Appl Environ Micro.* 2014;80:2110–9.
29. Jepson BJN, Marietou A, Mohan S, Cole JA, Butler CS, Richardson DJ. Evolution of the soluble nitrate reductase: defining the monomeric periplasmic nitrate reductase subgroup. *Biochem Soc T.* 2006;34:122–6.
30. Haase D, Hermann B, Einsle O, Simon J. Epsilonproteobacterial hydroxylamine oxidoreductase (epsilon Hao): characterization of a 'missing link' in the multi-haem cytochrome c family. *Mol Microbiol.* 2017;105:127–38.
31. Klotz MG, Schmid MC, Strous M, op den Camp HJ, Jetten MS, Hooper AB. Evolution of an octahaem cytochrome c protein family that is key to aerobic and anaerobic ammonia oxidation by bacteria. *Environ Microbiol.* 2008;10:3150–63.
32. Betlach MR, Tiedje JM. Kinetic explanation for accumulation of nitrite, nitric-oxide, and nitrous-oxide during bacterial denitrification. *Appl Environ Micro.* 1981;42:1074–84.
33. Simon J, Klotz MG. Diversity and evolution of bioenergetic systems involved in microbial nitrogen compound transformations. *BBA Bioenerg.* 2013;1827:114–35.
34. Hermans M, Lenstra WK, Hidalgo-Martinez S, van Helmond N, Witbaard R, Meysman FJR, et al. Abundance and biogeochemical impact of cable bacteria in Baltic sea sediments. *Environ Sci Technol.* 2019;53:7494–503.
35. Marshall IPG, Starnawski P, Cupit C, Fernandez Caceres E, Ettema TJG, Schramm A, et al. The novel bacterial phylum Calditrichaeota is diverse, widespread and abundant in marine sediments and has the capacity to degrade detrital proteins. *Environ Microbiol Rep.* 2017;9:397–403.
36. Lefevre CT, Frankel RB, Abreu F, Lins U, Bazyliński DA. Culture-independent characterization of a novel, uncultivated magnetotactic member of the Nitrospirae phylum. *Environ Microbiol.* 2011;13:538–49.
37. Logares R, Brate J, Bertilsson S, Clasen JL, Shalchian-Tabrizi K, Rengefors K. Infrequent marine-freshwater transitions in the microbial world. *Trends Microbiol.* 2009;17:414–22.
38. Trojan D, Schreiber L, Bjerg JT, Boggild A, Yang T, Kjeldsen KU, et al. A taxonomic framework for cable bacteria and proposal of the candidate genera *Electrothrix* and *Electronema*. *Syst Appl Microbiol.* 2016;39:297–306.
39. Dam AS, Marshall IPG, Risgaard-Petersen N, Burdorf LDW, Marzocchi U. Effect of salinity on cable bacteria species composition and diversity. *Environ Microbiol.* 2021;23:2605–16.
40. Jones CM, Stres B, Rosenquist M, Hallin S. Phylogenetic analysis of nitrite, nitric oxide, and nitrous oxide respiratory enzymes reveal a complex evolutionary history for denitrification. *Mol Biol Evol.* 2008;25:1955–66.
41. Graf DR, Jones CM, Hallin S. Intergenomic comparisons highlight modularity of the denitrification pathway and underpin the importance of community structure for N₂O emissions. *PLoS ONE.* 2014;9:e114118.
42. Kraft B, Strous M, Tegetmeyer HE. Microbial nitrate respiration - Genes, enzymes and environmental distribution. *J Biotechnol.* 2011;155:104–17.
43. Simon J, Sängler M, Schuster SC, Gross R. Electron transport to periplasmic nitrate reductase (NapA) of *Wolinella succinogenes* is independent of a NapC protein. *Mol Microbiol.* 2003;49:69–79.
44. Bjerg JT, Boschker HTS, Larsen S, Berry D, Schmid M, Millo D, et al. Long-distance electron transport in individual, living cable bacteria. *Proc Natl Acad Sci USA.* 2018;115:5786–91.
45. Venceslau SS, Lino RR, Pereira IAC. The Qrc membrane complex, related to the alternative complex III, is a menaquinone reductase involved in sulfate respiration. *J Biol Chem.* 2010;285:22774–83.
46. Meysman FJR, Risgaard-Petersen N, Malkin SY, Nielsen LP. The geochemical fingerprint of microbial long-distance electron transport in the seafloor. *Geochim Cosmochim Acta.* 2015;152:122–42.
47. Kern M, Simon J. Electron transport chains and bioenergetics of respiratory nitrogen metabolism in *Wolinella succinogenes* and other Epsilonproteobacteria. *Biochim Biophys Acta.* 2009;1787:646–56.
48. Chen Y, Wang F. Insights on nitrate respiration by *Shewanella*. *Front Mar Sci.* 2015; 1:80.
49. Gao H, Yang ZK, Barua S, Reed SB, Romine MF, Neelson KH, et al. Reduction of nitrate in *Shewanella oneidensis* depends on atypical NAP and NRF systems with NapB as a preferred electron transport protein from CymA to NapA. *ISME J.* 2009;3:966–76.
50. Geerlings NMJ, Karman C, Trashin S, As KS, Kienhuis MVM, Hidalgo-Martinez S, et al. Division of labor and growth during electrical cooperation in multicellular cable bacteria. *Proc Natl Acad Sci USA.* 2020;117:5478–85.
51. Scilipoti S, Koren K, Risgaard-Petersen N, Schramm A, Nielsen LP. Oxygen consumption of individual cable bacteria. *Sci Adv.* 2021; 7:eabe1870.
52. Bjerg JT, Damgaard LR, Holm SA, Schramm A, Nielsen LP. Motility of electric cable bacteria. *Appl Environ Microbiol.* 2016;82:3816–21.
53. Dam A-S, Marshall IPG, Petersen NR, Burdorf LDW, Marzocchi U. Effect of salinity on cable bacteria species composition and diversity. *Environ Microbiol.* 2021;23:2605–16.
54. Westram R, Bader K, Pruesse E, Kumar Y, Meier H, Glöckner FO, et al. ARB: a software environment for sequence data. In: de Bruijn FJ, editor. *Handbook of molecular microbial ecology I: metagenomics and complementary approaches.* John Wiley & Sons, Inc.; Hoboken, New Jersey; 2011. p. 399–406.

ACKNOWLEDGEMENTS

We are grateful to Lars B. Pedersen for microsensor construction, to Jeanette Johansen, Susanne Nielsen, and Karina B. Oest for help with laboratory analysis. Tage Dalsgaard is acknowledged for support to the isotopic analysis, and Filip Meysman, David Richardson, Tom Clarke, and Andrew Gates for fruitful and inspirational discussion. Results incorporated in this study have received funding from the European Union's Horizon 2020 research and innovation program under the Marie Skłodowska-Curie grant agreement No 656385 (U.M.), the Grundfos Foundation (U.M.); and the Danish National Research Foundation (grant DNRF104; NR-P, A.S.).

COMPETING INTERESTS

The authors declare no competing interests.

ADDITIONAL INFORMATION

Supplementary information The online version contains supplementary material available at <https://doi.org/10.1038/s41396-021-01048-z>.

Correspondence and requests for materials should be addressed to U.M.

Reprints and permission information is available at <http://www.nature.com/reprints>

Publisher's note Springer Nature remains neutral with regard to jurisdictional claims in published maps and institutional affiliations.